

Direct measurement of evolving dark energy density and re-accelerating expansion of the universe

Shuang-Nan Zhang^{1,2*} and Yin-Zhe Ma^{3,4}

¹Key Laboratory for Particle Astrophysics, Institute of High Energy Physics, CAS, 19B Yuquan Road, Beijing 100049, China

²National Astronomical Observatories of China, CAS, 20A Datun Road, Beijing 100020, China

³Department of Physics and Astronomy, University of British Columbia, Vancouver, BC, Canada and

⁴Canadian Institute for Theoretical Astrophysics, Toronto, Ontario, Canada

(Dated: December 2, 2024)

A higher value of Hubble constant has been obtained from measurements with nearby Type Ia supernovae, than that obtained at much higher redshift. With the peculiar motions of their hosts, we find that the matter content at such low redshift is only about 10% of that at much higher redshifts; such a low matter density cannot be produced from density perturbations in the background of the Λ CDM expansion. Recently the *Planck* team has reported a lower Hubble constant and a higher matter content. We find that the dark energy density increases with cosmic time, so that its equation-of-state parameter decreases with cosmic time and is less than -1 at low redshift. Such dark energy evolution is responsible for driving the re-accelerating expansion of the universe. In this extended Λ CDM model, the cosmological redshift represents time rather than radial coordinate, so that the universe complies to the Copernican Principle.

PACS numbers: 98.80.Es

The Hubble constant H_0 measures the expansion rate of present day universe, provides the basic information on the age of the universe, and is a key parameter related to other cosmological parameters, such as densities of dark matter (DM) and dark energy (DE) in the universe. H_0 can be determined by measuring the Hubble parameter $H(z) \equiv \dot{a}/a$ at any redshift z and then projecting it to $z = 0$ with an underlying cosmological model, where a is the scale factor of the universe at z . Therefore H_0 determined this way is model-dependent, unless $z \approx 0$. In the following, $H_{0,z}$ denotes the Hubble constant projected with measurements at z . This means, in principle, only $H_{0,0}$ is model-independent. The best model-independent measurement of $H_{0,0}$ can be made using nearby Type Ia supernovae (SNe Ia), which are currently the best standard candles in cosmology from the local universe to $z \simeq 1$. Recently a 3.3% error of $h_{0,0} = 0.738$ ($h \equiv H/100 \text{ km s}^{-1} \text{ Mpc}^{-1}$) is reported by calibrating these standard candles with many Cepheid variables in their host galaxies [1], which are the best distance indicators of the local universe. This result is consistent with that obtained directly with Cepheid variables, but bypassing the uncertainties in the distance to the Large Magellanic Cloud [2].

Currently the standard cosmology model is the base Λ CDM model, in which the cold DM and DE (Λ) dominate the matter and energy contents of the universe and the DE density does not change with cosmic time. Decisive evidence for the existence of DE was found from comparisons between the apparent magnitudes of the low- and high- z SNe Ia, which led the discovery of the accelerating expansion of the universe [3, 4]. The projected H_0 with the base Λ CDM model should be the same from measurements made at all z , if the base Λ CDM model describes the properties of the universe at all z with universal parameters. For example, the DE density $\rho_\Lambda \equiv 3H_0^2\Omega_\Lambda/8\pi G$ should remain the same from measurements made at all z , since H_0 and Ω_Λ are universal parameters in the base Λ CDM model. For convenience we define the normalized DE parameter $\Psi_{\Lambda,z} = \Omega_{\Lambda,z}h_{0,z}^2$, where $\Omega_{\Lambda,z}$

and $h_{0,z}$ are obtained with measurements at z ; we then have $\rho_{\Lambda,z} = \frac{3 \times \tilde{H}_0^2}{8\pi G} \Psi_{\Lambda,z}$, where $\tilde{H}_0 = 100 \text{ km s}^{-1} \text{ Mpc}^{-1}$. Since $\rho_{\Lambda,z}$ does not vary in the base Λ CDM model, $\rho_{\Lambda,z}$ obtained by fitting data with the base Λ CDM model is actually the DE density at redshift z . Therefore the base Λ CDM model provides a convenient framework to determine directly the evolution of DE density, if it describes the universe at each epoch accurately. Since observationally we normally measure $\Omega_{M,z}h_{0,z}^2$ at z , we re-write $\Psi_{\Lambda,z} = (1 - \Omega_{M,z})h_{0,z}^2$, for a flat universe ($\Omega_K = 0$). Recently, the *Planck* mission has released its results as $h_{0,z} = 0.679 \pm 0.015$ and $\Omega_{M,z}h^2 = 0.1423 \pm 0.0029$ (at $z \sim 1100$) [5]. As we will show in this paper, both of them are different from the low redshift measurements of SNe Ia with high statistical significance, requiring an increasing DE density with cosmic time.

Indeed, just before the discovery of the accelerating expansion of the universe [3, 4], evidence was found that $H_{0,0} > H_{0,z}$ ($z \gtrsim 0.01$) by about 6%, where the boundary is around $D_L \sim 70 h^{-1} \text{ Mpc}$ [7]. This suggests that we are living within a small local Hubble bubble, which expands slightly faster than the outside universe. Therefore we are moving away with respect to distant SNe Ia faster than the global Hubble expansion and thus the distant SNe Ia should look dimmer than viewing only within the Hubble flow. This has led heated debate if the accelerating expansion of the universe is simply an mirage of this local Hubble bubble, i.e., we are living in a local void model [8–16], since the over-dimming of distant SNe Ia is what led to the initial discovery of the accelerating expansion of the universe. However in the base Λ CDM model (with $\rho_{\Lambda,z} = \text{const}$), the $H_{0,0}$ parameter should be considered a global property of the universe, and can be used directly as a pre-determined parameter when constraining the other cosmological parameters with cosmic microwave background observations ($z \sim 1100$) [17]. As we will show in this paper, neither model agrees with the SNe Ia data with $z \gtrsim 0.01$ and thus the void model is rejected and the base

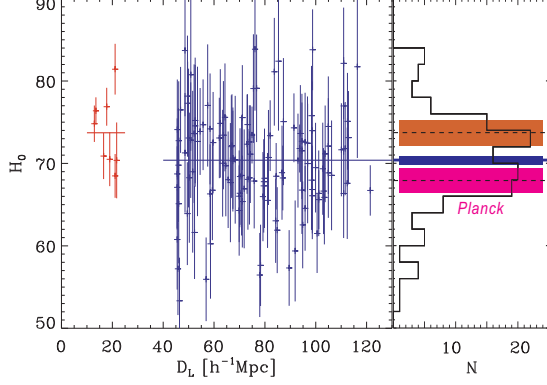


FIG. 1: The Hubble constant h_0 measured with each SNe Ia within a luminosity distance D_L of $250 \text{ h}^{-1}\text{Mpc}$. **Left panel:** The red crosses are the eight best SNe Ia [1] used to measure the local H_0 with $D_L < 25 \text{ h}^{-1}\text{Mpc}$, giving an average local $h_{0,0} = 0.738 \pm 0.0155$ marked as the thick solid red line. The blue crosses are the Union 2.1 SNe Ia [6] at $D_L > 40 \text{ h}^{-1}\text{Mpc}$, yielding an average $h_{0,z_{1-}} = 0.704 \pm 0.0051$ as the thick solid blue line ($z_{1-} = 0.025$ is the median redshift of these SNe Ia marked by the blue crosses). Seven of the eight SNe Ia (red crosses) have $h_0 > h_{0,z_{1-}}$, indicating that the probability that the eight SNe Ia are drawn from the same population of the other SNe Ia (blue crosses) is less than 3.6%. The null hypothesis that the two samples have the same mean is rejected at 96.3% confidence level with Welch's t -test. **Right panel:** Histogram of the blue crosses in the left panel. The filled red and blue areas are the 1σ error regions of $h_{0,0}$ and $h_{0,z_{1-}}$ respectively; their errors are calculated from the variance of each sample, and are significantly larger than that calculated from error propagation using the measurement errors of all data points (see text for details). The large error in $h_{0,0}$ is due to its very small sample size of only eight data points and additional fluctuations caused by the peculiar motions of their hosts (see text for details). $h_{0,0}$ and $h_{0,z_{1-}}$ are different at 2.1σ level with respect to their joint error bar, i.e., the probability that they are consistent with each other is less than 3.6%. For comparison, the just released *Planck* result $h_{0,z_2} = 0.679 \pm 0.015$ is also marked by the filled magenta area ($z_2 \sim 1100$).

Λ CDM model should be extended by allowing evolving DE density with cosmic time.

Similar to the previous work [7], in Figure 1 we show H_0 measured from the currently best available SNe Ia data, i.e. the eight SNe Ia ($z = 0.0043$ to 0.0072) [1] to obtain $H_{0,0}$ and the Union 2.1 compilation [6] to measure $H_{0,z}$. The data for the eight SNe Ia are listed in Table 1 in the supplementary material; h_0 (with standard error σ_{h_0}) is calculated by using Equation (4) and data in Table 3 of Ref.[1]. h_0 for other SNe Ia is calculated using the standard method, e.g., Equation (12) or (13) in Ref.[18] with the same choices of parameters. We limit the SNe Ia with $z < 0.04$ (with a median redshift of $z_{1-} = 0.025$), in order to avoid any coupling with cosmological parameters; in fact it is already safe to choose $z < 0.1$ [18]. We obtain $h_{0,0} = 0.738 \pm 0.0155$ and $h_{0,z_{1-}} = 0.704 \pm 0.0051$, and $h_{0,0} > h_{0,z_{1-}}$ at 96.4% confidence level (CL) (see the figure caption for details). Since our goal here is to examine the statistical consistency between

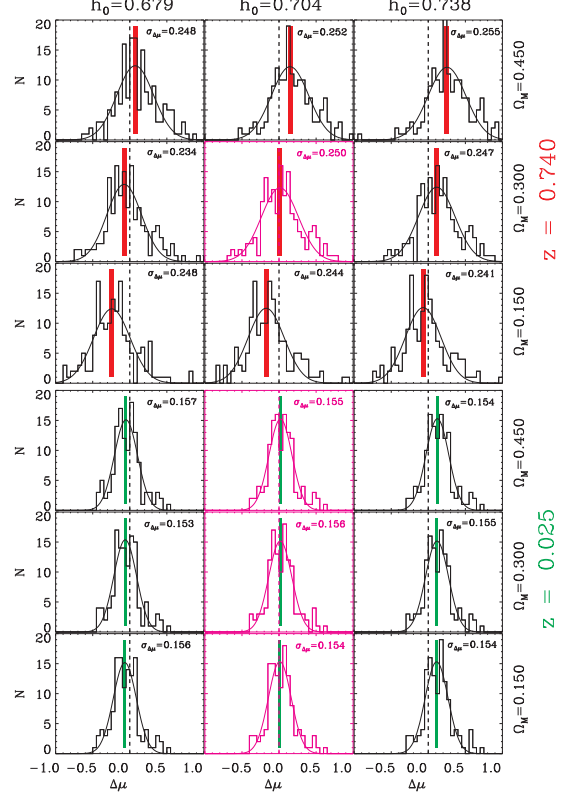


FIG. 2: Residuals of the distance modules (μ) of the Union 2.1 SNe Ia against the prediction of the Λ CDM cosmological model with different combinations of Ω_M and H_0 ; $\Omega_M + \Omega_\Lambda = 1$ is always assumed. The black thick vertical dashed lines indicate $\Delta\mu = 0$. Two groups of SNe Ia are chosen here: low redshift of $z \leq 0.04$ with a median redshift of 0.025 , and high redshift of $z \geq 0.5$ with a median redshift of 0.740 . The combination of the absolute value of $\widehat{\Delta\mu}$ (the center of the distribution of $\Delta\mu$) and the magnitude of $\sigma_{\Delta\mu}$ (the standard deviation of each Gaussian fit, also labelled in each panel), indicates how well the model describes the data. Each filled area marks the 3σ error range of $\widehat{\Delta\mu}$ with $\sigma_{\widehat{\Delta\mu}} = \sigma_{\Delta\mu}/\sqrt{n-1}$, where n is the total number of data points. The four panels plotted in magenta color are consistent with data: $h_0 = 0.704$ for $z_{1-} = 0.025$, independent of Ω_M ; also $h_0 = 0.704$ for $z_{1+} = 0.740$, unless Ω_M deviates significantly from 0.3 .

the two values of h_0 , only statistical errors in these SNe Ia are included here; the effects of possible larger errors in $h_{0,0}$, including cosmic variance, are discussed later. This confirm the previous result [7] with the most updated and best available data. For comparison, we also show $h_{0,z_2} = 0.679 \pm 0.015$ ($z_2 \sim 1100$) in Figure 1, reported by the *Planck* team [5].

In Figure 2, we examine critically if the three values of the Hubble constant, i.e., $h_{0,0}$, $h_{0,z_{1-}}$ and h_{0,z_2} , are consistent with the Union 2.1 SNe Ia data at both low and high redshift, within the framework of the base Λ CDM model with different values of (but not evolving) Ω_M . We conclude that only $h_0 = 0.704$ is consistent with data at low redshift ($z_{1-} = 0.025$), independent of Ω_M . At high redshift ($z_{1+} = 0.740$), again only $h_0 = 0.704$ is consistent with data

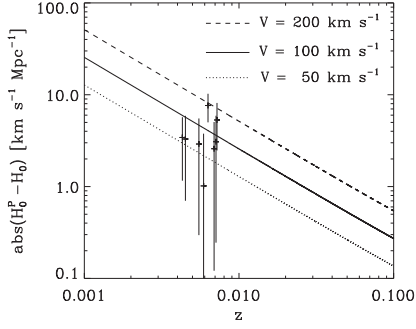


FIG. 3: Deviations of the measured H_0 with individual SNe Ia, caused by the peculiar motions of SNe Ia hosts at different redshift. The lines are the expected deviations for different peculiar velocities along the LOS. The data points with error bars are the deviations of the eight SNe Ia from $h_{0,0} = 0.738$. The data are consistent with the LOS peculiar velocity of about 100 km s^{-1} .

unless Ω_M deviates significantly from around 0.3; actually the high redshift SNe Ia data favors a lower value of $\Omega_M = 0.28$. It is thus very unlikely that SNe Ia data can be reconciled with either the higher or lower h_0 measured in the local bubble or with the cosmic microwave background data of *Planck*, respectively. Therefore the combined SNe-Ia and *Planck* data support an increasing $h_{0,z}$ with increasing cosmic time or decreasing z . A remaining issue is whether the higher value of $h_{0,0}$ is just due to a density perturbation in the local universe, i.e., we are living in a local density void embedded in an otherwise uniform expansion of the universe described by the base Λ CDM model. In such a scenario, the under-density is given by $-\Delta\Omega_M/\Omega_M = 2\Delta h_0/h_0 \approx 0.1$.

The matter density Ω_M in the bubble can be measured by the peculiar velocity dispersion of these SNe Ia hosts. From each listed $H_{0,0}$ and its error in Table 1, the pure statistical error of $h_{0,0}$ should be 0.009, much smaller than the error of 0.0155 determined from the variance of the eight data points. This means that the probability that the data do not contain additional fluctuations is less than 0.68%. It has been known that the peculiar motions of the SNe Ia hosts may cause such fluctuations beyond the measurement statistical errors [19, 20]. Since $H_0 \cong cz/D_L$ when $z \cong 0$, a non-negligible deviation to H_0 may be produced for a peculiar velocity along the line of sight (LOS) $V_{\text{los}} \sim 100 \text{ km s}^{-1}$ at $z \ll 1$. The additional fluctuations caused by the random peculiar motions of the SNe Ia hosts can be found from $\sigma_{h_{0,P}}^2 = \langle h_0^2 \rangle - \bar{\sigma}_{h_0}^2 = 0.0352^2$, where $\langle h_0^2 \rangle = \sum (h_{0,i} - \bar{h}_0)^2 / (n-1)$ and $\bar{\sigma}_{h_0} = \sum \sigma_{h_{0,i}} / n = 0.0262$ ($n = 8$); in fact $\bar{\sigma}_{h_0} \simeq \sigma_{h_{0,i}}$. Clearly $\sigma_{h_{0,P}} > \bar{\sigma}_{h_0}$, i.e., the average fluctuation to h_0 caused by the putative random peculiar motions of SNe Ia hosts is larger than the measurement errors in h_0 .

We then compare the measured $|H_{0,i} - \bar{H}_0|$ with the expected deviations caused by different LOS peculiar velocities at low redshift in Figure 3; here $\bar{H}_0 = H_{0,0}$. The data are consistent with $V_{\text{los}} \sim 100 \text{ km s}^{-1}$. In Figure 1 of the supplementary material, we show the positions of the eight SNe Ia in

equatorial coordinates and their LOS peculiar velocities from the Hubble flow with $H_{0,0}$; the detected peculiar motions do not show any significantly coordinated pattern (albeit with small number statistics) and thus are consistent with random motions with respect to the Hubble flow; this also agrees with the previous conclusion [7]. For random peculiar motions, the commonly measured pairwise velocity dispersion between the eight SNe Ia is found to be $\hat{\sigma}_{12} = 141 \pm 26.5 \text{ km s}^{-1}$ (1σ range); here the effects of the measurement errors of each V_{los} and the sample size have been considered (Please refer to the supplementary material for details). The projected separations between these pairs are between 5 to $40 h^{-1} \text{ Mpc}$ (see the supplementary material for details). It has been shown that $\hat{\sigma}_{12}$ converges to 500 km s^{-1} (for $\Omega_M = 0.3$, $\hat{\sigma}_{12} \propto \Omega_M^{0.55}$) at these separations, with almost no luminosity dependence [21]. Therefore the observed peculiar velocities of the eight SNe Ia suggest that the local matter density $\Omega_{M,0} = 0.030 \pm 0.011$. We thus have $-\Delta\Omega_M/\Omega_M \sim 0.9 \gg 2\Delta h_0/h_0 \approx 0.1$. This discrepancy cannot be reconciled even if the possible cosmic variance effect is considered on the uncertainty of $h_0 = 0.738$ with an additional $\sim 2.5\%$ [22]. Actually a slightly lower value than $h_0 = 0.738$ will make the discrepancy even larger, and a slightly higher value than $h_0 = 0.738$ will make it farther away from $h_0 = 0.704$ but still lower than that required by the under-density in the bubble.

Therefore the void model is excluded with high significance. Actually the spherically symmetric but inhomogeneous Lemaître-Tolman-Bondi (LTB) model of the universe has been excluded with stringent limits [13, 23–25]. As a straightforward and simple extension to the base Λ CDM model, the local bubble with $h_0 = 0.738$ and $\Omega_M \sim 0.03$ can be considered as the global property of present day universe; observationally it becomes “local” because only a small volume of present day universe can be observed by any observer, due to the limited light propagation. In other words, an observer located anywhere in the universe at $z \sim 0$, with respect to the cosmic microwave background at $z \sim 1100$, should also observe the same local bubble. This is good news, since it naturally avoids the philosophical crisis if we are living in a specially chosen place in the universe, i.e., the center of the universe where the matter density is much lower than the rest of the universe.

More specifically, the SNe Ia and *Planck* data support a scenario that the universe expands initially at a low rate (at $z \sim 1100$), then slightly higher rate (at $z \lesssim 1$), and finally even higher rate at present day (at $z \sim 0$), i.e., the projected Hubble constant $h_{0,z}$ increases with cosmic time. We call this *re-accelerating expansion of the universe*, to distinguish it from the well-known accelerating expansion of the universe described by the base Λ CDM model, with a constant DE density and a constant Hubble constant [3, 4]. The normalized DE densities at the three redshifts can be obtained directly as: $\Psi_{\Lambda,0} = 0.53^{+0.21}_{-0.10}$ ($z_0 \sim 0$), $\Psi_{\Lambda,z_1} = 0.357^{+0.029}_{-0.014}$ ($z_1 \sim 1$), and $\Psi_{\Lambda,z_2} = 0.103^{+0.082}_{-0.040}$ ($z_2 \sim 1100$); all errors quoted here are for 95% CL.

Matter and DE are completely decoupled in the Λ CDM

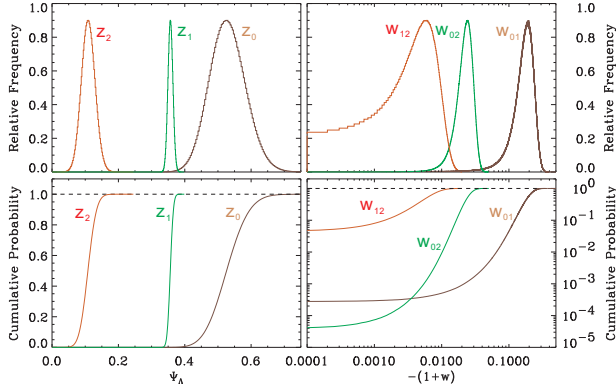


FIG. 4: The normalized DE density Ψ_Λ and DE equation-of-state parameter w obtained from measurements at three redshifts: $z_0 \sim 0$, $z_1 \sim 1$, and $z_2 \sim 1100$. Input parameters with 1σ -errors are: $h_{0,0} = 0.703 \pm 0.0352$ (i.e., 5% error in $h_{0,0}$), $\Omega_{M,0} = 0.030 \pm 0.011$, $h_{0,z_1} = 0.704 \pm 0.0051$, $\Omega_{M,z_1} = 0.28 \pm 0.01$, $h_{0,z_2} = 0.679 \pm 0.015$ and $\Omega_{M,z_2} h_{0,z_2}^2 = 0.1423 \pm 0.0029$. The cases for smaller errors in h_0 are discussed in the supplementary material; just one percent improvement in the precision to h_0 can improve the accuracy of w considerably.

model, therefore the energy conservation for DE requires $\rho_\Lambda \propto a^{-3(1+w)}$, where w is the DE equation-of-state parameter. The cosmological model is commonly referred to as w CDM model, if w is allowed to deviate from -1 , as an extension to the base Λ CDM model. With measurements of Ψ_Λ made at any two redshifts z_i and z_j ($z_i < z_j$), we have $3(1+w_{z_i,z_j}) = -\log(\Psi_{\Lambda,z_i}/\Psi_{\Lambda,z_j})/\log((1+z_j)/(1+z_i))$. We therefore obtain: $-(w_{z_0,z_1} + 1) = 0.188^{+0.194}_{-0.102}$, $-(w_{z_0,z_2} + 1) = 0.024^{+0.022}_{-0.011}$, and $-(w_{z_1,z_2} + 1) = 0.0060^{+0.014}_{-0.0068}$, respectively. Therefore at 95% CL, both w_{z_0,z_1} and w_{z_0,z_2} are less than -1 ; w_{z_1,z_2} is just marginally consistent with -1 . The probability distributions of Ψ_Λ and w are shown in Figure 4. Therefore the observed increasing DE density with cosmic time found here requires $w < -1$ with high statistical significance (the so-called phantom DE) at low- z and w decreases with cosmic time. In this case the cosmological redshift z can be interpreted as the time coordinate t (clock of the universe) rather than radial coordinate r , and thus the universe can still maintain homogeneous and comply with the Copernican Principle, unless there is large scale anisotropy in any observable (See the supplementary material for more details, including a new LTB(t) scheme).

The extremely low matter density at $z = 0.0043$ to 0.0072 seems to contradict the measured over-density just outside our local group [26]. However, previous surveys of the nearby galaxies have found that the baryon density (Ω_b) declines very rapidly beyond the local group and is already half of the cosmological average at about $6 h^{-1}\text{Mpc}$ [27], where it is still well inside the local supercluster. It is physically plausible that Ω_b outside the local supercluster continues to decline by a factor a few, in agreement with our measured very low Ω_M in the local bubble, if baryon matter also traces DM halos in

present day universe. This may explain naturally the missing baryon problem at low- z . We thus predict that the majority of the low- z (local) baryon matter is not bounded by DM halos, but is distributed between galaxies as intergalactic medium.

The measured PVD with 2dF and galaxy luminosity density at low- z are consistent with $\Omega_{M,z} \sim 0.2$ at $z \lesssim 0.1$ [21, 28]. Different compilations of SNe Ia data, joint fits between CMB data (*Planck* or *WMAP*) with other observations (including lensing and BAO) all support a picture of $\Omega_{M,z}$ increasing with z . This also explains why the *Planck* results are consistent BAO data but not with SNe Ia data, due to the fact the BAO measures mostly Ω_{M,z_2} and h_{0,z_2} ($z_2 \sim 1100$), though observed at very low- z . Interestingly, the comparison between *Planck*+BAO and *WMAP*+BAO also suggests that the discrepancy between *Planck* and *WMAP* results may be due to systematics in the *WMAP* data. (Please see the supplementary material for extensive discussions on all issues in this paragraph.)

Many cosmological probes, such as PVD, galaxy counts and luminosity function, clusters of galaxies, lensing, etc, can only measure DM content in cosmic structures. On the other hand, standard candles (e.g. SNe Ia peak luminosity) and standard rules (e.g. BAO scale) measure effectively the average DM content in the universe. Therefore $\Omega_{M,0} = 0.030 \pm 0.011$ at $z \ll 1$, inferred from PVD of SNe Ia hosts, might indicate that the local DM is mostly not contained in DM halos, but distributed uniformly as a background of the local universe, in a similar way to the missed local baryons in cosmic structures. A significant amount of uniformly distributed DM at low- z is, however, not expected at all in cold or even warm-DM models. Unfortunately, there is currently no effective way to measure the average matter density in the local universe.

SNZ is grateful to Drs. Hong Li and Yu-Zhong Wu who helped me in collecting the data used in this work. Xuelei Chen, Yipeng Jing, Tipei Li, Weipeng Lin, Richard Lieu, Roger Penrose, David Valls-Gabaud, Junqing Xia, Marcel Zemp, Bing Zhang and Pengjie Zhang are thanked for discussions, comments or suggestions. SNZ acknowledges partial funding support by 973 Program of China under grant 2009CB824800, by the National Natural Science Foundation of China under grant Nos. 11133002 and 10725313, and by the Qianren start-up grant 292012312D1117210.

* Electronic address: zhangsn@ihp.ac.cn

- [1] A. G. Riess, *et al.*, *The Astrophysical Journal* **730**, 119 (2011).
- [2] A. G. Riess, J. Fliri, D. Valls-Gabaud, *The Astrophysical Journal* **745**, 156 (2012).
- [3] A. G. Riess, *et al.*, *The Astronomical Journal* **116**, 1009 (1998).
- [4] S. Perlmutter, *et al.*, *The Astrophysical Journal* **517**, 565 (1999).
- [5] Planck Collaboration I, P. A. R. Ade, *et al.* (2013) (arXiv:1303.5062).
- [6] N. Suzuki, *et al.*, *The Astrophysical Journal* **746**, 85 (2012).
- [7] I. Zehavi, A. G. Riess, R. P. Kirshner, A. Dekel, *The Astrophysical Journal* **503**, 483 (1998).

- [8] H. Alnes, M. Amarzguioui, O. Grøn, *Physical Review D* **73**, 083519 (2006).
- [9] S. Alexander, T. Biswas, A. Notari, D. Vaid, *Journal of Cosmology and Astroparticle Physics* **2009**, 025 (2009).
- [10] T. Mattsson, *General Relativity and Gravitation* **42**, 567 (2009).
- [11] M. Mortonson, W. Hu, D. Huterer, *Physical Review D* **80**, 067301 (2009).
- [12] B. Sinclair, T. M. Davis, T. Haugbølle, *The Astrophysical Journal* **718**, 1445 (2010).
- [13] A. Moss, J. P. Zibin, D. Scott, *Physical Review D* **83**, 103515 (2011).
- [14] G. F. R. Ellis, *Classical and Quantum Gravity* **28**, 164001 (2011).
- [15] S. Nadathur, S. Sarkar, *Physical Review D* **83**, 063506 (2011).
- [16] V. Marra, A. Notari, *Classical and Quantum Gravity* **28**, 164004 (2011).
- [17] G. Hinshaw, *et al.* (2012) (arXiv:1212.5226).
- [18] A. G. Riess, *et al.*, *The Astrophysical Journal* **699**, 539 (2009).
- [19] L. Hui, P. Greene, *Physical Review D* **73**, 123526 (2006).
- [20] P. Zhang, X. Chen, *Physical Review D* **78**, 023006 (2008).
- [21] J. L. Tinker, P. Norberg, D. H. Weinberg, M. S. Warren, *The Astrophysical Journal* **659**, 877 (2007).
- [22] V. Marra, L. Amendola, I. Sawicki, W. Valkenburg (2013) (arXiv:1303.3121).
- [23] P. Zhang, A. Stebbins, *Physical Review Letters* **107**, 041301 (2011).
- [24] J. P. Zibin, A. Moss, *Classical and Quantum Gravity* **28**, 164005 (2011).
- [25] F. Y. Wang, Z. G. Dai (2013) (arXiv:1304.4399).
- [26] D. Schlegel, M. Davis, F. Summers, J. A. Holtzman, *The Astrophysical Journal* **427**, 527 (1994).
- [27] I. D. Karachentsev, V. E. Karachentseva, W. K. Huchtmeier, D. I. Makarov, *The Astronomical Journal* **127**, 2031 (2004).
- [28] R. C. Keenan, *et al.*, *The Astrophysical Journal* **754**, 131 (2012).

Supplementary material

1. Data and sky map of the eight SNe Ia

Table 1 lists all data of the eight SNe Ia used in this work. Figure 1 plots in the sky map the positions and LOS velocities of the eight SNe Ia, which are consistent with random and isotropic distribution (albeit with small number statistics).

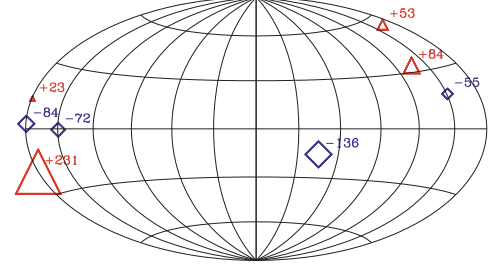


FIG. 1: Positions of the eight SNe Ia in equatorial coordinates and their LOS peculiar velocities from the Hubble flow. Negative (marked as blue diamonds) and positive (marked as red triangles) velocities mean that their hosts are moving towards and away from the observer within the Hubble flow with $h_{0,0} = 0.738$, respectively. The sizes of the signs are proportional to their LOS velocity deviations.

2. Pairwise velocity dispersion

The apparent pairwise velocity dispersion is calculated between the eight SNe Ia as

$$\sigma_{12}^2 = \sum_{i,j} (V_{\text{los},i} - V_{\text{los},j})^2 / N, \quad (1)$$

where $i = 1$ to 7 , $j = i + 1$ to 8 , and $N = 28$ is the total number of pairs. The distribution of the projected separations of these pairs is shown in Figure 2. The true pairwise velocity dispersion should be given by

$$\hat{\sigma}_{12}^2 = \sigma_{12}^2 - 2\sigma_0^2, \quad (2)$$

where $\sigma_0 = 63.8 \text{ km s}^{-1}$ is the average measurement error in $V_{\text{los},i}$.

For this small sample of peculiar velocities with measurement errors, we perform Monte-Carlo simulations to evaluate the expected values of the pairwise velocity dispersion and its error. A random sample of $V_{\text{los},i}$ is produced with a Gaussian distribution of zero mean and standard deviation σ . Then for each random group of eight $V_{\text{los},i}$, σ_{12} is calculated with equation (1). The distribution of σ_{12} and its cumulative probability distribution are shown in Figure 3; $\sigma = 122.5 \text{ km s}^{-1}$ is chosen so that the observed $\sigma_{12} = 167.2 \text{ km s}^{-1}$ equals the mean value of the simulated distribution. With equation (2), we have $\hat{\sigma}_{12} = 141 \pm 26.5 \text{ km s}^{-1}$ (1σ range). For comparison, we also show the simulation results for 30 and 100 SNe Ia, which produce $\sigma(\hat{\sigma}_{12}) = 13$ and $\sigma(\hat{\sigma}_{12}) = 6$, respectively.

TABLE I: Redshift, coordinates (J2000.0), Hubble constant and LOS peculiar velocities of the eight SNe Ia.

Name	redshift	Right ascension (hh:mm:ss)	Declination (dd:mm:ss)	Hubble Constant H_0 (km s ⁻¹ Mpc ⁻¹)	LOS pec. vel. V_{los} (km s ⁻¹)
1981b	0.0072	12:34:29.57	+02:11:59.3	70.37 (2.26)	-84.7 (66.7)
1990n	0.0043	12:42:56.68	+13:15:23.4	74.81 (2.75)	23.3 (48.3)
1994ae	0.0045	11:56:25.87	+55:07:43.2	76.38 (2.46)	53.2 (45.1)
1998aq	0.0055	10:47:01.94	+17:16:30.8	70.89 (2.61)	-55.9 (58.6)
1995al	0.0059	09:50:55.97	+33:33:09.4	76.87 (2.83)	84.1 (68.1)
2002fk	0.0070	03:22:05.71	-15:24:03.2	68.48 (2.83)	-136.3 (81.1)
2007af	0.0070	12:01:52.80	-18:58:21.7	81.43 (2.62)	231.3 (75.0)
2007sr	0.0063	14:22:21.03	-00:23:37.6	70.50 (2.59)	-72.5 (66.8)

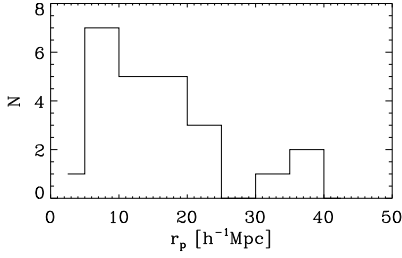
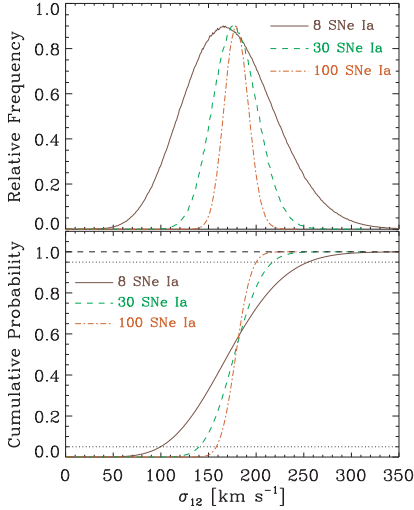


FIG. 2: Distribution of projected separations between the 28 pairs.

FIG. 3: Simulated distribution σ_{12} and its cumulative probability distribution, for the cases of 8, 30 and 100 SNe Ia, respectively.

3. Input parameters with errors and derived dark energy parameters

In Table 2, we list the input parameters for h_{0,z_i} and Ω_{M,z_i} and the derived the dark energy parameters in the paper.

4. Impacts of the error in h_0 and sample size

In Figure 4 of the main paper, we conservatively assumed a 5% error in h_0 , which is reasonable due to the reported 3.3% uncertainty [1] and a possible 2.5% uncertainty due to cosmic variance [2]. To understand the impacts of the error in h_0 to the inferred dark energy parameters, in Figures 4 and 5, we show the derived distributions of normalized dark energy density Ψ_Λ and equation-of-state parameter w . We can see dramatic improvements even if the error in h_0 is reduced by an additional 1%.

For completeness, we also simulated the cases for samples of 30 and 100 SNe Ia, in order to overcome the possible error in $\hat{\sigma}_{12}$ caused by the small sample size of only eight SNe Ia in the current study. However, only very marginal improvements are expected even if the sample size is increased to 100, although the uncertainties to $\hat{\sigma}_{12}$ are significantly reduced, in proportion to $1/\sqrt{n}$, where n is the sample size. This is because $\Omega_{M,0}$ is so small, that the dominant factor in determining $\Psi_{\Lambda,0} = (1 - \Omega_{M,0})h_{0,0}^2$ is $h_{0,0}$. However, a larger sample will improve the statistical accuracy in $h_{0,0}$, again in proportion to $1/\sqrt{n}$, which will results in better determination of $\Psi_{\Lambda,0}$.

5. Discussions on BAO measurements

5.1 Simplified case

The Baryon Acoustic Oscillation (BAO) observations measure the acoustic sound horizon size d_H at the last scattering surface ($z_L = z_2 \sim 1100$), where the Cosmic Microwave Background (CMB) radiation is produced. With the base Λ CDM model and assuming that the cosmological parameters are the same from infinite redshift to redshift to z_L , we have [3]

$$d_H = \frac{2}{H_{0,z_L} \sqrt{3R_L \Omega_{M,z_L} (1+z_L)^3} \ln\left(\frac{\sqrt{1+R_L} + \sqrt{R_{EQ} + R_L}}{1 + \sqrt{R_{EQ}}}\right)}, \quad (3)$$

TABLE II: Input parameters with errors and derived dark energy parameters.

$z_0 \sim 0$		$z_1 \sim 1$		$z_2 \sim 1100$	
$10^2 \cdot h_{0,0}$	$10^2 \cdot \Omega_{M,0}$	$10^2 \cdot h_{0,z_1}$	$10^2 \cdot \Omega_{M,z_1}$	$10^2 \cdot h_{0,z_2}$	$10^2 \cdot \Omega_{M,z_2} h_{0,z_2}^2$
70.3 ± 3.52	3 ± 1.1	70.4 ± 0.51	28 ± 1	67.9 ± 1.5	14.23 ± 0.29
$\Psi_{\Lambda,0} = 0.53^{+0.21}_{-0.10}$		$\Psi_{\Lambda,z_1} = 0.357^{+0.029}_{-0.014}$		$\Psi_{\Lambda,z_2} = 0.103^{+0.082}_{-0.040}$	
$-(w_{z_0,z_1} + 1) = 0.188^{+0.194}_{-0.102}$		$-(w_{z_1,z_2} + 1) = 0.0060^{+0.014}_{-0.0068}$		$-(w_{z_0,z_2} + 1) = 0.024^{+0.022}_{-0.011}$	

Note: Errors for input parameters are all 1σ . Errors for Ψ_{Λ,z_i} and w_{z_i,z_j} are for 95% confident level.

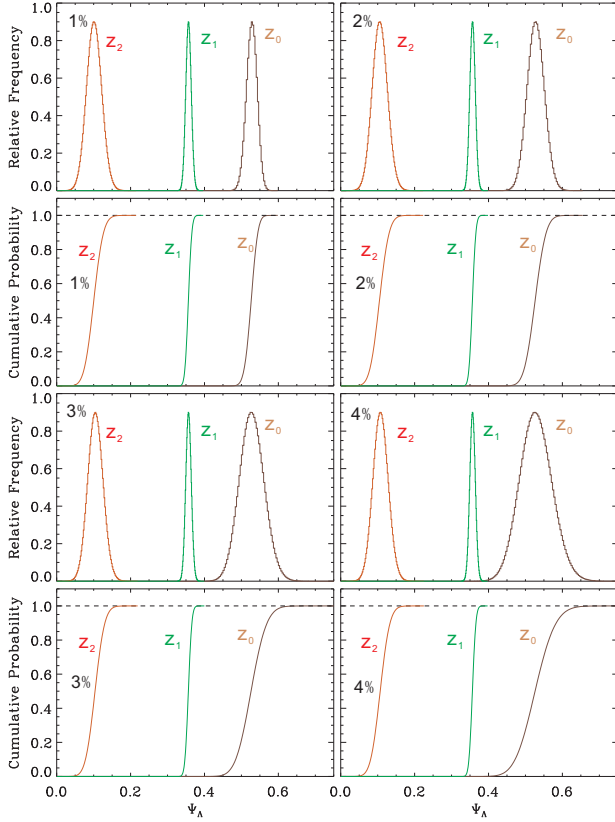


FIG. 4: The normalized dark energy density Ψ_Λ obtained from measurements at three redshifts ($z_0 \sim 0$, $z_1 \sim 1$, and $z_2 \sim 1100$) for different precisions of $h_{0,0}$. All other input parameters and errors are unchanged. Note that only $\Psi_{\Lambda,0}$ is changed.

where $R \equiv 3\rho_B/4\sigma T^4$, ρ_B is baryon density, and the subscripts 'L' and 'EQ' refer to the last scattering surface and matter-radiation equilibrium, respectively. Since $R_L \propto \Omega_B H_{0,z_L}^2$, we have (aside from a slowly varying logarithm) [3]

$$d_H \propto \Omega_B^{-1/2} \Omega_{M,z_L}^{-1/2} h_{0,z_L}^{-2}. \quad (4)$$

Therefore what BAO observations really measure are the cosmological parameters projected to $z = 0$ from the last scattering surface, i.e., the same as that with CMB observations.

However, in order to obtain the BAO scale at a certain redshift z , the angular diameter distance at z must be calculated,

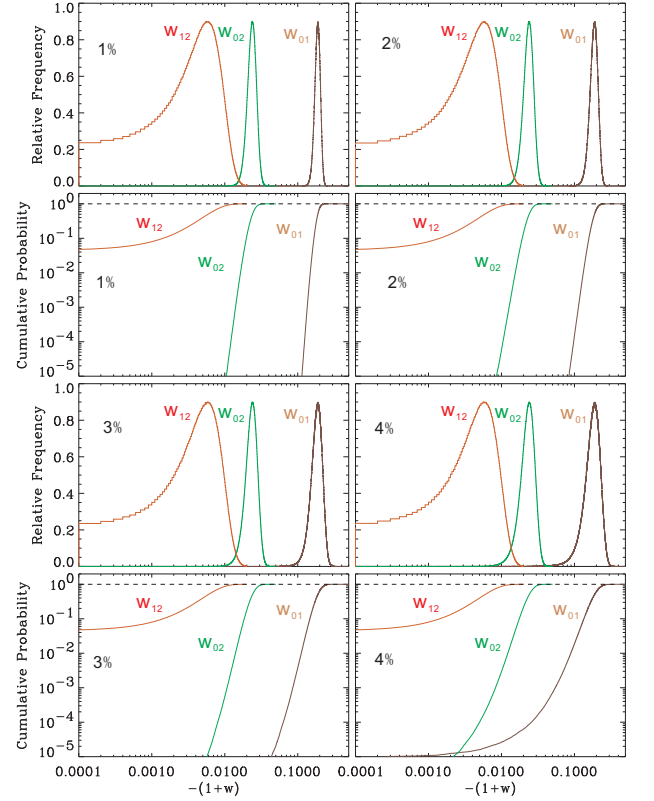


FIG. 5: The dark energy equation-of-state parameter w obtained from measurements at three redshifts ($z_0 \sim 0$, $z_1 \sim 1$, and $z_2 \sim 1100$) for different precisions of $h_{0,0}$. All other input parameters and errors are unchanged. Note that $w_{1,2}$ is unchanged.

which depends on the cosmological parameters from zero redshift to z . For simplicity, we assume that the cosmological parameters (again in the base Λ CDM model) are the same from zero redshift to z . The angular diameter distance is then given by,

$$D_A = \frac{c}{H_{0,z}(1+z)} \int_0^z \frac{dz'}{\sqrt{\Omega_{M,z}(1+z')^3 + \Omega_{K,z}(1+z')^2 + \Omega_{\Lambda,z}}}. \quad (5)$$

Therefore BAO data are connected to cosmological parameters both at redshift from zero to z and at redshift from z_L

to infinity. With BAO measurements alone, it is in principle not possible to obtain cosmological parameters at both ends, due to the degeneracy discussed above. However, combining with other low redshift data (such as SNe Ia data discussed in this work), it is easy to break the degeneracy and to obtain cosmological parameters at higher than z_L , which can be then compared with CMB results.

It is easy to find: $-\partial \ln d_H / \partial \ln h_{0,z_L} = 2$, $-\partial \ln D_A / \partial \ln h_{0,z} = 1$, $-\partial \ln d_H / \partial \ln \Omega_{M,z_L} = 0.5$; $-\partial \ln D_A / \partial \ln \Omega_{M,z} < 0.3$ for $z < 1$, as shown in Figure 6 for $\Omega_{M,z} = 0.2$ and 0.3 ($\Omega_K = 0$ is assumed), respectively. This demonstrates that the BAO observations are always more sensitive to h_{0,z_L} than to $h_{0,z}$, and are more sensitive to Ω_{M,z_L} than to $\Omega_{M,z}$ when $z \lesssim 1$.

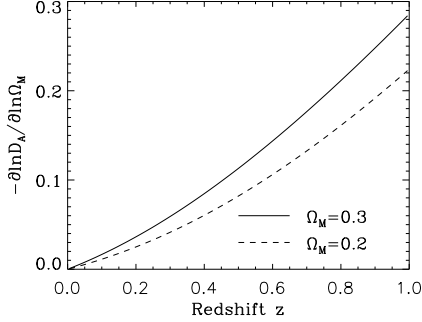


FIG. 6: Dependence of angular diameter distance on Ω_M at different redshift; $\Omega_K = 0$ is assumed.

5.2 Realistic case

Realistically, we need to consider the logarithm term in equation (3), the difference between the drag epoch (z_d) and the epoch at the last scattering surface (z_L), and the fact that BAO measurements are always obtained within a certain spherical volume of redshift z , which can be taken into account by the spherically averaged D_A , i.e., D_V . Therefore what BAO experiments actually measure is $r_s(z_d)/D_V(z)$ (Ref.[4]). We use Eqs. (1)-(6) in Ref.[5] to calculate r_s and $D_V(z)$. Similar to the simplified case, we again take logarithmic derivative to parameters Ω_M and h_0 ; the results are shown in Figure 7.

One can see that $-\partial \ln r_s(z_d)/\partial \ln \Omega_{M,z_L} = 0.248$ and $-\partial \ln r_s(z_d)/\partial \ln h_{0,z_L} = 0.895$, consistent to the previously used (e.g., Eq. (12) of Ref.[6])

$$r_s(z_d) \propto \Omega_M^{-0.255} h_0^{-0.778}, \quad (6)$$

which is quite different from Eq. (4) for the simplified case discussed above. Nevertheless, similarly to the simplified case, our details calculation also shows $-\frac{\partial \ln r_s(z_d)}{\partial \ln \Omega_{M,z_L}} > -\frac{\partial \ln D_V(z_1)}{\partial \ln \Omega_{M,z}}$ and $-\frac{\partial \ln r_s(z_d)}{\partial \ln h_{0,z_L}} > -\frac{\partial \ln D_V(z)}{\partial \ln h_{0,z}}$ ($z < 1$); therefore connecting $D_V(z)$ directly to $r_s(z_d)$, i.e., assuming

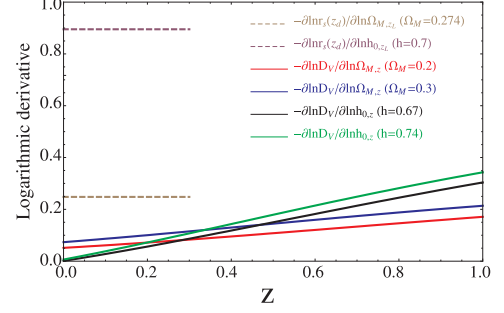


FIG. 7: Dependence of r_s and $D_V(z)$ on Ω_M and h_0 ; $\Omega_K = 0$ is assumed.

$D_V(z) \propto r_s(z_d)$, actually probes Ω_{M,z_L} and h_{0,z_L} much more sensitively than to $\Omega_{M,z}$ and $h_{0,z}$ ($z < 1$), unless $\Omega_{M,z_L} = \Omega_{M,z}$ and $h_{0,z_L} = h_{0,z}$, as assumed implicitly in previous studies.

Since all existing BAO observations are made to $z < 1$, the above analyses explain naturally why h_0 and Ω_M obtained with BAO data are consistent with CMB results, but not with SNe Ia results with data at even similar redshifts. Nevertheless BAO data are connected to cosmological parameters (Ω_M and h_0 here) at both z_L and at low- z . In fact, the combined-BAO derived $H_0 = 68.4^{+1.0}_{-1.0}$ and $\Omega_M = 0.305^{+0.009}_{-0.008}$ (the last row in Table 8 of Ref.[7]) are between that of SNe Ia and *Planck*-only results but are closer to the latter, in support to our above analysis.

6. Low redshift matter density

In the paper, we have assumed the matter density $\Omega_{M,z_1} = 0.28 \pm 0.01$, which is consistent with the high- z ($z > 0.5$) Union 2.1 SNe Ia data and has been well-accepted in the concordance Λ CDM model prior to the *Planck* result. Both CMB and BAO data contribute significantly to this value, since it has been assumed so far that globally there is a unique Ω_M . However, neither CMB nor BAO data should be used to measure uniquely Ω_{M,z_1} , as discussed above.

There are still many other cosmological probes that can be used to measure Ω_{M,z_1} , such as galaxy counts, galaxy luminosity functions, weak gravitational lensing, peculiar velocities of galaxies inferred from redshift space distortion with two-point correlation function, standard candles or rulers, etc. However galaxy counts and galaxy luminosity functions are known to be biased probes of matter density, due to redshift-dependent galaxy formation processes. On the other hand, weak gravitational lensing and peculiar velocities probe directly the gravitational field, and are thus neither biased nor redshift-dependent, when used to probe the matter density. Standard candles (such as SNe Ia) or rulers (such as BAO) have been extensively discussed above.

6.1 Joint fits between CMB and other data

It is instructive to inspect how the best fit of Ω_M changes, by combining CMB temperature power-spectrum with other probes. In Table 3, we compile such a list from *Planck* results [7] for easy comparison. From this table, we notice the following:

1. For the first two groups on the *Planck* data, i) all combinations results in lower Ω_M , higher h_0 and Ψ_Λ , consistent with our model that the dark energy density increases with cosmic time; ii) the percentages of changes are larger when combined with lensing, SNLS, or HST data; this is understandable since these data are only connected to low- z cosmological parameters; iii) the combination with Union2 data has the smallest change, even smaller than that with BAO data. The last one can also be understood, because there are 29 SNe Ia with $z > 1$ in the Union2 data, in comparison to only 11 SNe Ia with $z > 1$ in the SNLS data and for all BAO data $z < 1$. Therefore Union2 data probe Ω_M at higher redshift than all other data, except the CMB data. Consequently these results suggest that $\Omega_{M,z}$ decreases with decreasing z (or increasing cosmic time), once again fully consistent with our scenario.
2. For the last group on the *WMAP* data, i) aside from the BAO combination, the signs of changes are the same as the first two groups, but the fractions of changes are far more significant, which can be understood since the signal-to-noise ratios of the *WMAP* data are far less than that of the *Planck* data, such that the *WMAP* data play less significant roles in determining the joint fitting results; ii) for the BAO combination, the signs of changes are opposite to that on the *Planck* data, inconsistent with our analysis that BAO data should find slightly lower Ω_M and higher h_0 . Therefore we suggest that the discrepancy between *WMAP* and *Planck* data on Ω_M and h_0 may be due to systematic errors in *WMAP* data analysis. As a matter of fact, previous independent re-analysis [8] of *WMAP* data have found consistent results with that released recently by the *Planck* team.

6.2 SNe Ia data

In Figure 19 of Ref.[7], the best fit Ω_M is found to increase from SNLS, to Union2 and *Planck* data, consistent with the fact that these data probe Ω_M with increasing redshift. Therefore $\Omega_{M,z_1} = 0.28$ ($z_1 \sim 1$) is a reasonable choice, determined with the Union2 data. On the other hand, it is quite possible that the SNLS data probe Ω_M at lower redshift more sensitively, with $\Omega_{M,z} = 0.23$ at $z \sim 0.5$.

6.3 Peculiar velocities from 2dF survey

In Figure 6 of Ref.[9], the distribution of pairwise peculiar velocity dispersion (PVD) of galaxies in the 2dF survey is compared with high-resolution N -body simulation. The

TABLE III: Matter density and Hubble constant obtained with different combinations of data in the base Λ CDM model [7]. The first row of each group lists values of the best-fit parameters, below which are the relative changes of these parameters in percentage when combined with other data. The last column is the normalized dark energy density defined in this paper: $\Psi_\Lambda \equiv \Omega_\Lambda h_0^2 = (1 - \Omega_M)h_0^2$ (for $\Omega_K = 0$).

Data	Ω_M	H_0	$\Omega_M h_0^2$	Ψ_Λ
lowL+lowLike	0.318300	67.0400	0.143050	0.306386
+ lensing (%)	-4.71254	1.67065	-1.49598	5.64073
+ BAO (%)	-2.51336	0.880066	-0.789933	2.96209
+ HST (%)	-5.46654	1.96897	-1.71269	6.63307
+ SNLS (%)	-3.58153	1.25298	-1.15345	4.23755
+ Union2 (%)	-1.53943	0.551913	-0.433420	1.82602
lowL+lowLike+highL	0.317000	67.1500	0.142970	0.307942
+ lensing (%)	-3.43848	1.17647	-1.16108	4.00467
+ BAO (%)	-2.64984	0.923299	-0.888296	3.12879
+ HST (%)	-4.76341	1.66790	-1.58075	5.65917
+ SNLS (%)	-3.47003	1.20625	-1.15408	4.08967
+ Union2 (%)	-1.45110	0.506324	-0.489611	1.71384
<i>WMAP</i>	0.292000	68.8700	0.138400	0.335908
+ BAO (%)	1.84932	-0.580807	0.794800	-1.96292
+ HST (%)	-10.0685	3.81878	-2.96243	12.2109
+ SNLS (%)	-15.1712	4.82068	-5.46965	15.8555
+ Union2 (%)	-11.6096	3.57195	-4.16907	11.7333

Notes: **lowL**: low- l *Planck* temperature ($2 \leq l \leq 49$); **highL**: high- l *Planck* temperature (CamSpec, $50 \leq l \leq 2500$); **lensing**: *Planck* lensing power spectrum reconstruction; **lowLike**: low- l *WMAP* 9 polarization; **BAO**: Baryon oscillation data from DR7, DR9 and 6dF; **SNLS**: Supernova data from the Supernova Legacy Survey; **Union2**: Supernova data from the Union compilation; **HST**: Hubble parameter constraint from HST (Riess et al. [1]); **WMAP**: The full *WMAP* (temperature and polarization) 9 year data.

flattening of the observed PVD to about 450 km s^{-1} to the projected separations above several Mpc is consistent with $\Omega_M = 0.2$. Since the median redshift of the 2dF survey is 0.1, this result suggest that $\Omega_{M,z} = 0.2$ at $z \sim 0.1$, again suggesting increasing Ω_M with redshift.

7. Local matter density

In the paper, we have found a very low local matter density $\Omega_{M,0} = 0.03 \pm 0.011$ at about $20 h^{-1} \text{Mpc}$, i.e., just outside our local group. Here we examine critically if this is consistent with other observations.

Local galaxy counts within $5 h^{-1} \text{Mpc}$ show an over-density of about 25%, compared to the cosmological average [10]. This may argue for an over-density in the total local mass distribution. However, this is not in conflict with our conclusion of low Ω_M in present day universe, since the over-density is just outside the local group and well-within the local supercluster, where the mean matter density should be higher than the cosmological average. The total baryon mass density derived from the most complete nearby galaxy catalogue

is $\Omega_B = 0.023$ within about $6 h^{-1}\text{Mpc}$, about half of the cosmological average [11]. Since the mean HI density decreases rapidly at larger distances (Figure 14 of Ref. [11]), it is physically plausible that Ω_B decreases by a factor of a few at about $20 h^{-1}\text{Mpc}$, i.e., nearly to the boundary of the local supercluster. Therefore $\Omega_{M,0} = 0.03 \pm 0.011$ outside the local supercluster does not conflict the data of nearby galaxy data, if baryon to total mass ratio remains about the same as the cosmological average. Actually the very low PVD of about 100 km s^{-1} of these galaxies within about $6 h^{-1}\text{Mpc}$ at projected separations of below and around $1 h^{-1}\text{Mpc}$ also supports a very low value of Ω_M .

In Figure 6 of Ref. [12], a significant lower luminosity density of galaxies is found at redshift between 0.02 to 0.07, compared to that above redshift of 0.1. Even after considering possible cosmic variance, a significant lower mass density at redshift below 0.1 cannot be excluded [12]. This is also consistent with a significantly lower mass density in present day universe discussed above.

The data shown above, from high redshift to low redshift, all support a picture that $\Omega_{M,z}$ increases with z . On the other hand, at low redshift regime, baryonic matter traces the dark matter halos, so $\Omega_{B,0}$ measured in cosmic structures should be also much lower than the global value. Since the total baryon is conserved, this indicates that at low redshift and present day Universe, most baryonic matter is not bounded by dark matter halos and thus distributed between galaxies as intergalactic medium. This scenario provides a natural explanation of the missing baryon problem and can be tested with future observations.

8. $\Lambda\text{LTB}(t)$ scheme

Our main conclusion is that the dark energy density increases with cosmic time, in a way that its equation-of-state parameter decreases with cosmic time and is less than -1 at low redshift. However, currently there is no well-understood physics to account for the dark energy evolving this way.

If matter and dark energy are coupled, then phenomenologically the increasing dark energy density would require decreasing matter content in the universe. A class of models, referred to as unified or coupled dark matter and dark energy models, have been widely studied in literature, such as the generalized Chaplygin gas model [13] or gravity-dark energy coupling model [14]. Unfortunately both models generally require a rapid increase of $\rho_\Lambda(z)$ with z , opposite to our result. Our results that $\rho_\Lambda(z)$ increases with cosmic time seems to imply that dark matter is continuously converted to dark energy and the conversion rate only increases rapidly at low- z , which drives the observed re-accelerating expansion of the universe. Mathematically a cosmological model of universe with time varying parameters can be described with the LTB metric including the dark energy term Λ , the so-called ΛLTB

metric. We name this class of models as $\Lambda\text{LTB}(t)$ models, to distinguish them from the ΛLTB models commonly used to describe a spherically symmetric, but spatially inhomogeneous universe, i.e., $\Lambda\text{LTB}(r)$ models. Here we suggest a specific $\Lambda\text{LTB}(t)$ scheme in which the time varying parameter is $\rho_\Lambda(z)$ (or $\Psi_{\Lambda,z}$). Within this framework, the ΛCDM model can be used to describe the universe at any epoch of cosmic time.

A generic property of a $\text{LTB}(t)$ model (with or without Λ) is that cosmological redshift z is interpreted as the time coordinate t (clock of the universe) rather than radial coordinate r . Therefore there is no such concept as radial inhomogeneity in a $\text{LTB}(t)$ model; any previously observed radial dependence of any cosmological parameter or physical quantities (even in the comoving frame) is interpreted as evolutionary effects in a $\text{LTB}(t)$ model. In principle simultaneous events can only be observed between two points in the universe with the same redshift (i.e. in the transverse direction), unless any evolutionary effect is negligible. The Copernican Principle is naturally maintained, since in a $\text{LTB}(t)$ model any observer anywhere in the universe observes at the same cosmic time the same thing in the universe. The Copernican Principle can be violated only if cosmological parameters or measured physical quantities show large scale anisotropy; in this case the spherical symmetry in the LTB prescription is broken. Therefore $\text{LTB}(t)$ models can be falsified by any observed large scale anisotropy.

* Electronic address: zhangsn@ihep.ac.cn

- [1] A. G. Riess, *et al.*, *The Astrophysical Journal* **730**, 119 (2011).
- [2] V. Marra, L. Amendola, I. Sawicki, W. Valkenburg (2013) (arXiv:1303.3121).
- [3] S. Weinberg, *Cosmology* (Oxford University Press, Oxford, England, 2008).
- [4] G. Hinshaw, *et al.* (2012) (arXiv:1212.5226).
- [5] E. Komatsu, *et al.*, *The Astrophysical Journal Supplement Series* **180**, 330 (2009).
- [6] W. J. Percival, *et al.*, *Monthly Notices of the Royal Astronomical Society* **401**, 2148 (2010).
- [7] Planck Collaboration XVI, P. Bielewicz, *et al.* (2013) (arXiv:1303.5076).
- [8] H. Liu, T.-P. Li (2009) (arXiv:0907.2731).
- [9] J. L. Tinker, P. Norberg, D. H. Weinberg, M. S. Warren, *The Astrophysical Journal* **659**, 877 (2007).
- [10] D. Schlegel, M. Davis, F. Summers, J. A. Holtzman, *The Astrophysical Journal* **427**, 527 (1994).
- [11] I. D. Karachentsev, V. E. Karachentseva, W. K. Huchtmeier, D. I. Makarov, *The Astronomical Journal* **127**, 2031 (2004).
- [12] R. C. Keenan, *et al.*, *The Astrophysical Journal* **754**, 131 (2012).
- [13] M. Bento, O. Bertolami, A. Sen, *Physical Review D* **66**, 043507 (2002).
- [14] T.-P. Li, M. Wu (2013) (arXiv:0907.2731).